



Fusing Porphyrins and Phospholes: Synthesis and Analysis of a Phosphorus-Containing Porphyrin

Tomohiro Higashino,* Tomoki Yamada, Tsuneaki Sakurai, Shu Seki, and Hiroshi Imahori*

Abstract: A phosphole-fused porphyrin dimer, as a representative of a new class of porphyrins with a phosphorus atom, was synthesized for the first time. The porphyrin dimer exhibits remarkably broadened absorption, indicating effective π -conjugation over the two porphyrins through the phosphole moiety. The porphyrin dimer possesses excellent electron-accepting character, which is comparable to that of a representative electron-accepting material, [60]PCBM. These results provide access to a new class of phosphorus-containing porphyrins with unique optoelectronic properties.

Porphyrins are macrocyclic 18π -conjugated molecules that have been actively studied in various fields owing to their potential for diverse applications, for example, in materials science and as catalysts, as well as owing to their vital roles in natural systems.^[1] As their attractive properties are attributed to the 18π electron conjugated system, their structural and electronic properties can be tuned by metalation, peripheral modification, and replacement of a pyrrole ring with another heterocycle.^[2,3] In particular, the chemistry of porphyrins with phosphorus atoms has been actively investigated in the light of the ability of the phosphorus atom to form coordination and covalent bonds (Figure 1). For instance, phosphorus-containing porphyrin complexes can be used as a structural motif to create oligomeric architectures. The wheel-and-axle phosphorus(V) porphyrin arrays **1** were synthesized by Shimidzu and co-workers.^[4] Furthermore, phosphorus insertion has recently been shown to be an effective approach for creating new porphyrinoids.^[5] Latos-Grażyński and co-workers reported the phosphorus complex of N-fused porphyrin **2**, a 20π porphyrin, as an isophlorin analogue.^[5a] As another example, peripherally phosphanylated porphyrins have also been synthesized, which can form peripherally metalated porphyrins.^[6] The PCP pincer complexes of bis(phosphanyl)porphyrin **3** were catalytically active depending on the central metal atom in the porphyrin core.^[6c]

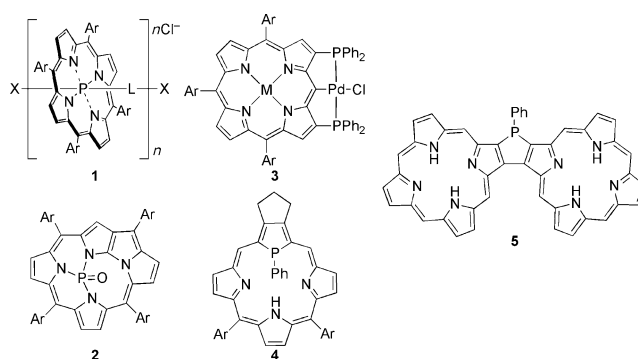


Figure 1. Examples of porphyrins with phosphorus atoms.

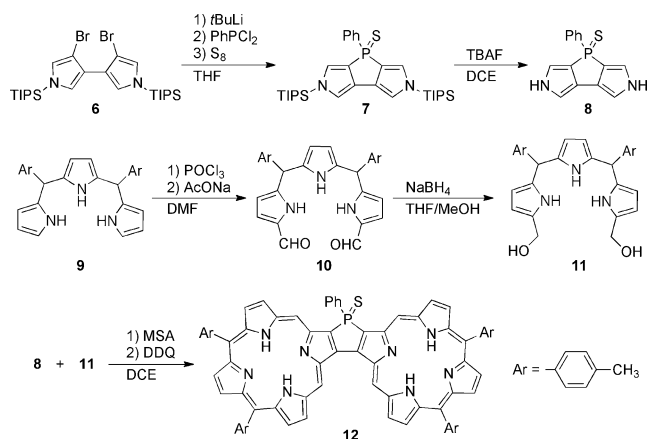
Phosphaporphyrins **4** have been presented by Matano and co-workers as core-modified porphyrins containing a phosphole ring.^[7] They corroborated that replacement of a pyrrole ring with a phosphole has an impact on the structure, aromaticity, and optical and electrochemical properties as well as on the coordination abilities. However, to the best of our knowledge, no porphyrins with a peripherally fused phosphole structure such as **5** have been reported in spite of extensive efforts to explore various phosphole-fused π -conjugated molecules.^[8] We envisioned that such phosphole-fused porphyrins would exhibit unique optical and electrochemical properties owing to the phosphole moiety. Towards this goal, we exploited a new synthetic method to create bis(pyrrolo)heteroles.^[9] On the basis of the reactivity of bis(pyrrolo)phosphole as a key building block, we expected that the two porphyrin rings would be integrated through condensation with the bis(pyrrolo)phosphole. Herein, we report for the first time the synthesis of phosphole-fused porphyrin dimers as a new class of porphyrins with a phosphorus atom.

The phosphole-fused porphyrin dimer **12** was synthesized by the route shown in Scheme 1. The treatment of 4,4'-dibromo-3,3'-bipyrrole **6**^[9] with *t*-BuLi and PhPCl_2 followed by addition of elemental sulfur afforded the triisopropylsilyl-protected bis(pyrrolo)phosphole **7** in 58 % yield. Whereas the P^{III} derivative is unstable under ambient atmosphere,^[9] the P^{V} compound **7** is sufficiently stable to be used as the precursor. Then, **7** was deprotected with tetrabutylammonium fluoride (TBAF) to give bis(pyrrolo)phosphole **8**. The reaction of 5,10-di(4-methylphenyl)tripyrane **9** with Vilsmeier reagent provided diformyltripyrane **10** in 52 % yield. Tripyrane dicarbinol **11** was obtained by the reduction of **10** with NaBH_4 . Then, we attempted the acid-catalyzed condensation of **8** and **11**. However, we detected only a trace amount of **12** under standard reaction conditions for porphyrin synthesis. After extensive screening, we finally succeeded in isolating the

[*] Dr. T. Higashino, T. Yamada, Dr. T. Sakurai, Prof. Dr. S. Seki, Prof. Dr. H. Imahori
Department of Molecular Engineering
Graduate School of Engineering, Kyoto University
Nishikyo-ku, Kyoto, 615-8510 (Japan)
E-mail: t-higa@scl.kyoto-u.ac.jp
imahori@scl.kyoto-u.ac.jp

Prof. Dr. H. Imahori
Institute for Integrated Cell Material Sciences (WPI-iCeMS)
Kyoto University, Nishikyo-ku, Kyoto, 615-8510 (Japan)

Supporting information and the ORCID identification number(s) for the author(s) of this article can be found under:
<http://dx.doi.org/10.1002/anie.201607417>.



Scheme 1. Synthesis of phosphole-fused porphyrin dimer **12**. DCE = 1,2-dichloroethane, MSA = methanesulfonic acid, TBAF = tetrabutylammonium fluoride, TIPS = triisopropylsilyl.

desired porphyrin dimer **12** in 0.7 % yield upon condensation of **8** and **11** with 0.4 equiv of methanesulfonic acid (MSA) at 60 °C in 1,2-dichloroethane for 1 h followed by oxidation with 6 equiv of 2,3-dichloro-5,6-dicyanobenzoquinone (DDQ) at room temperature for 3 h. While the yield was low, we performed the synthesis repeatedly and obtained a sufficient amount of **12** for all measurements (ca. 10 mg). The high-resolution electrospray ionization time-of-flight (HR-ESI-TOF) mass spectrum of **12** exhibited a positive ion peak at m/z 1117.3936 (calcd for $C_{74}H_{54}N_8PS$: 1117.3924 $[M+H]^+$), which is consistent with the molecular structure of **12**. The 1H NMR spectrum of **12** in CD_2Cl_2 is shown in Figure 2. The

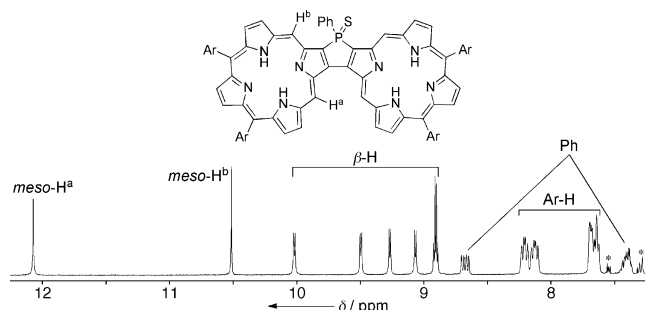


Figure 2. 1H NMR spectrum (aromatic region) of porphyrin dimer **12** in CD_2Cl_2 at 25 °C.

six resonances arising from the β -protons are observed in the range of δ = 8.90–10.03 ppm, and the two resonances arising from the meso protons are observed at δ = 10.51 and 12.07 ppm. It should be noted that the resonance of the meso- H^a protons is remarkably downfield-shifted because of the aromatic ring current of the neighboring porphyrin macrocycle. The ^{31}P NMR spectrum displays a resonance from the P=S moiety at δ = 18.76 ppm (see the Supporting Information, Figure S4).

To our delight, single crystals suitable for X-ray diffraction analysis were obtained by vapor diffusion of 2-propanol into a solution of **12** in 1,2-dichloroethane.^[10] The crystal structure

of **12** revealed two almost co-planar porphyrin macrocycles, which suggests effective π -conjugation over the two porphyrin moieties (Figure 3). Whereas porphyrin ring B adopts

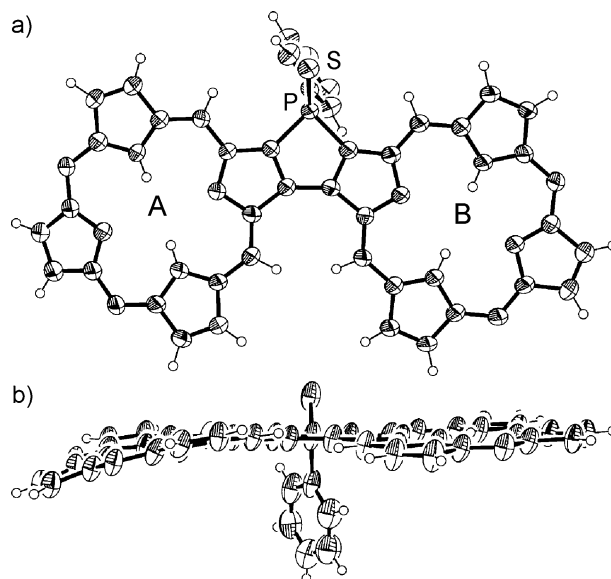


Figure 3. X-ray crystal structure of **12**: a) top view and b) side view. Thermal ellipsoids set at 50% probability. Solvent molecules and meso-aryl substituents omitted for clarity.

a highly planar conformation, a slight distortion was observed for porphyrin ring A. The mean-plane deviations (MPDs) of the porphyrin macrocycles A and B (24 core atoms) were calculated to be 0.234 and 0.035 Å, respectively. In the packing structure, **12** forms a face-to-face dimeric structure, in which the intermolecular distance is approximately 3.5 Å (Figure S5). Notably, this dimeric structure forms a slipped π - π -stacked structure (Figure S6). The distance between the two porphyrin substructures is also about 3.5 Å. This π - π interaction probably induces the distortion of porphyrin ring A in the packing structure. The dimeric structure and effective π - π interactions would be favorable for potential applications of **12** as a charge-transport material (see below).^[11]

The UV/Vis absorption spectra of **12** and 5,10-di(4-methylphenyl)porphyrin **13** in CH_2Cl_2 are shown in Figure 4. In contrast to porphyrin monomer **13**, porphyrin dimer **12** displays remarkably broadened absorption whereas the absorption coefficients of **12** at λ \approx 400 nm are smaller than those of **13**. The split Soret bands are broadened in the range of λ = 400–500 nm. The lowest-energy Q band of **12** (λ = 668 nm) is red-shifted by $\Delta\lambda$ = 43 nm relative to that of **13** (λ = 625 nm),^[12] and the absorption edge reaches to 700 nm. It is noteworthy that this red shift of the Q band for **12** is significantly larger than that for a usual β - β -linked porphyrin dimer ($\Delta\lambda$ = 8 nm).^[13] Thus these absorption features support an effective interaction between the two porphyrin macrocycles through the phosphole moiety. The steady-state fluorescence spectrum of **12** was recorded in CH_2Cl_2 , and an emission peak was detected at λ = 683 nm (Figure 4). The Stokes shift of **12** (330 cm^{-1}) is rather comparable to that of **13**

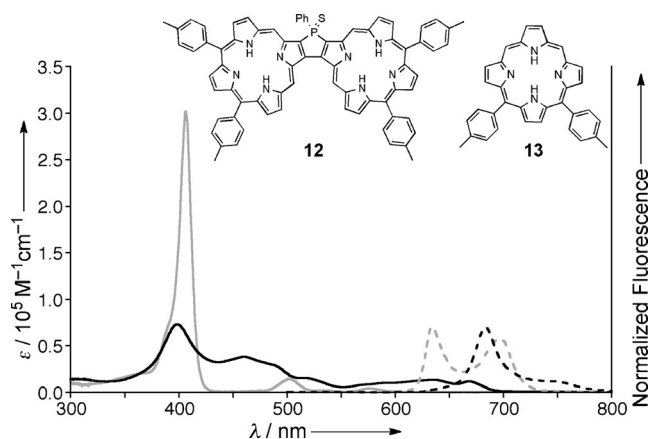


Figure 4. UV/Vis absorption (solid lines) and emission (dashed lines) spectra of **12** (black) and **13** (gray) in CH_2Cl_2 . The samples were excited at $\lambda = 400$ nm.

(230 cm^{-1}), which is consistent with the highly rigid planar structure of **12**.

The electrochemical properties of **7**, **12**, and **13** were studied by cyclic voltammetry (CV) and differential pulse voltammetry (DPV) in CH_2Cl_2 vs. ferrocene/ferrocenium cation (Fc/Fc^+) with tetrabutylammonium hexafluorophosphate (Bu_4NPF_6) as the electrolyte (Figure S7). Bis-(pyrrolo)phosphole **7** gave rise to an oxidation peak at 0.73 V whereas no reduction peak was visible at potentials up to -2.5 V. The electrochemical properties of **7** are similar to those of other bis-(pyrrolo)heteroles.^[9] Porphyrin monomer **13** displays two reversible reduction peaks at -1.65 and -2.05 V and two quasi-reversible oxidation peaks at 0.50 and 0.91 V. On the other hand, **12** underwent three quasi-reversible reductions at -1.19 , -1.44 , and -1.90 V and two irreversible oxidations at 0.53 and 0.75 V. The first and second oxidation potentials of **12** stem mainly from the two porphyrin moieties and the phosphole conjugated to the porphyrins, respectively (see below). The effective π -expansion over the two porphyrins lowers the oxidation potentials while they are shifted in the positive direction by the electron-withdrawing effect of the phosphorus(V) center, offsetting the effects; therefore, the oxidation potentials of **12** are comparable to those of **13** and **7**. In contrast, the three reduction peaks, including the unexpected new one, are significantly shifted in the positive direction, probably owing to the strongly electron-accepting character arising from the phosphole moiety (see below). The three one-electron reduction processes of **12** reflect distinct electronic communication over the two porphyrin moieties through the phosphole moiety. The large difference ($\Delta E_{\text{red}} = 0.25$ V) between the first and second reduction potentials also indicates effective electronic communication. It is worth noting that the first reduction potential of **12** is more positive than those of phosphole derivatives with high electron affinity.^[14] Given that the energy level of Fc/Fc^+ is -4.8 eV under vacuum, the LUMO level of **12** was estimated to be -3.61 eV.^[15] This value is close to that of [60]PCBM (ca. -3.7 eV),^[16] a representative fullerene derivative that is used as an electron-accepting material for charge transport as well as an organic photovoltaic material.^[17] Therefore, this high

electron-accepting ability, combined with effective π - π stacking in the crystal structure, suggests that **12** has potential as an n-type semiconductor.

To gain further insight into the electronic properties of **12**, we performed DFT calculations at the B3LYP/6-31G(d,p) level of theory. First, we found that **12a** is the most stable NH tautomer of **12** (Figure 5a). However, the difference in the

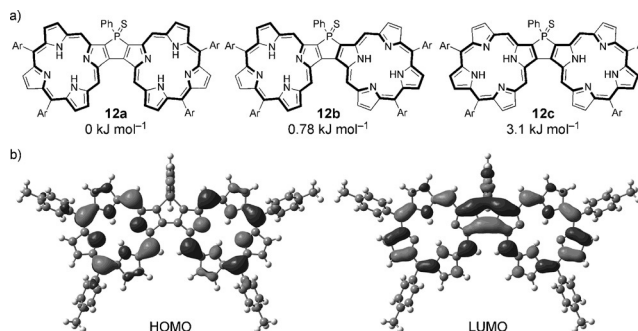


Figure 5. a) Three NH tautomers of **12** and their relative energies. b) Selected Kohn-Sham orbitals of **12a** at the B3LYP/6-31G(d,p) level of theory.

relative energies of the tautomers **12a–12c** is quite small (ca. 3 kJ mol^{-1}), which agrees with the single NH peak in the ^1H NMR spectrum of **12** at room temperature (Figure S4). The Kohn-Sham frontier orbitals of **12a** are illustrated in Figures 5b and S8. For the eight Kohn-Sham orbitals composed of four porphyrin orbitals, the orbital distributions are well delocalized over the whole π -conjugated system. HOMO and HOMO-1 of **12a** originate from the HOMO/HOMO-1 of **13**. As the phosphole ring is located on the node of HOMO/HOMO-1, these orbitals mainly exhibit porphyrin character. However, the energy levels of HOMO and HOMO-1 of **12a** are slightly shifted in the negative direction owing to the electron-withdrawing effect of the phosphorus(V) atom. On the other hand, the LUMO of **12a** is well delocalized over the two porphyrin moieties as well as the phosphole ring (Figure 5b). Importantly, the LUMO of **12a** is derived from the LUMO + 1 of **13** and remarkably stabilized compared to the LUMO + 1/LUMO + 2, which stem from the LUMO of **13** (Figure S8). The new reduction peak observed in the cyclic voltammogram was rationalized by the stabilized LUMO (Figure S7). As the LUMO displays a large orbital distribution on the phosphole ring, the LUMO possesses phosphole character to a large extent.^[8,14] This is a consequence of the stabilization solely by the fusion of the two porphyrins and the phosphole ring.

We also calculated nucleus-independent chemical shift (NICS) values for the optimized structure of **12a** (Figure S9). The NICS value at the center of the porphyrin moiety is -13.8 ppm, whereas the NICS value at the center of the phosphole ring is $+8.33$ ppm. This large positive NICS value results from the double diatropic ring current effect of the two porphyrin macrocycles. Although the phosphole ring can participate in π -conjugation with the two porphyrin moieties, it has little impact on the 18π aromatic character of the porphyrin moiety. Furthermore, we carried out time-depen-

dent DFT (TD-DFT) calculations to evaluate the absorption (Figure S10 and Table S2). The oscillator strengths of the HOMO/LUMO and HOMO-1/LUMO transitions are small ($f < 0.03$) whereas the HOMO-2/LUMO transition has a large oscillator strength ($f = 0.41$). These results suggest that the absorption at $\lambda = 600$ – 700 nm is not caused by intramolecular charge transfer (ICT) from the porphyrin core to the phosphole ring, but mainly by π – π^* transitions of the porphyrin dimer with phosphole moiety.

Finally, we assessed the charge-transport ability of **12** and **13** by flash photolysis time resolved microwave conductivity (FP-TRMC) measurements.^[18] The FP-TRMC profiles for drop-cast films of **12** and **13**, prepared from toluene solution, upon irradiation at $\lambda = 355$ nm are displayed in Figure S11, with a charge recombination rate constant high enough compared to the time constant of the measurement system (ca. 100 ns), especially for **12**. The maximum transient conductivity $(\phi\Sigma\mu)_{\max}$ for **13** was determined to be $6.5 \times 10^{-6} \text{ cm}^2 \text{ V}^{-1} \text{ s}^{-1}$, where ϕ and $\Sigma\mu$ are the charge carrier generation efficiency and the sum of the charge carrier mobilities. Importantly, the $(\phi\Sigma\mu)_{\max}$ value for **12** ($5.5 \times 10^{-5} \text{ cm}^2 \text{ V}^{-1} \text{ s}^{-1}$) is one order of magnitude larger than that for **13**. This remarkable difference is most likely due to the effective π – π interaction in the solid state, supporting the potential utility of the phosphole-fused structure as a charge-transport material.

In summary, we have reported the synthesis of phosphole-fused porphyrin dimer **12** as a representative of a new class of phosphorus-containing porphyrins, exemplifying the potential utility of our bis(pyrrolo)heteroles as building blocks for heterole-fused porphyrin dimers. Porphyrin dimer **12** exhibits effective π -conjugation over the two porphyrin macrocycles through the phosphole moiety. The low reduction potential of **12** is solely due to the integration of the two porphyrin moieties into one large π -system through the phosphole moiety. FP-TRMC measurements suggest the prospective use of **12** as a novel charge-transport material. The optical and electrochemical properties of the phosphole-fused porphyrin dimer could be tuned by further modifications of the phosphorus atom, metalation of the porphyrin core, or peripheral functionalizations. Furthermore, we believe that this report will enable the synthesis of new classes of porphyrins containing not only phosphorus but also other main-group elements, such as sulfur and silicon.

Acknowledgements

This work was supported by the JSPS (KAKENHI Grant Numbers 15K17822 (T.H.) and 25220801 (H.I.)). We thank Dr. Takayuki Tanaka and Prof. Atsuhiko Osuka (Kyoto University) for assistance with X-ray crystal structure analysis.

Keywords: main-group elements · phospholes · phosphorus · porphyrin dimers · porphyrinoids

How to cite: *Angew. Chem. Int. Ed.* **2016**, *55*, 12311–12315
Angew. Chem. **2016**, *128*, 12499–12503

- [1] a) *The Porphyrin Handbook*, Vol. 1–10 (Eds.: K. M. Kadish, K. M. Smith, R. Guilard), Academic Press, San Diego, **2000**; b) D. Gust, T. A. Moore, A. L. Moore, *Acc. Chem. Res.* **2001**, *34*, 40–48; c) D. Holten, D. F. Bocian, J. S. Lindsey, *Acc. Chem. Res.* **2002**, *35*, 57–69; d) H. Imahori, *J. Phys. Chem. B* **2004**, *108*, 6130–6143; e) M. Ethirajan, Y. Chen, P. Joshi, R. K. Pandey, *Chem. Soc. Rev.* **2011**, *40*, 340–362; f) T. Tanaka, A. Osuka, *Chem. Soc. Rev.* **2015**, *44*, 943–969; g) T. Higashino, H. Imahori, *Dalton Trans.* **2015**, *44*, 448–463.
- [2] a) B. M. J. M. Suijkerbuijk, R. J. M. Klein Gebbink, *Angew. Chem. Int. Ed.* **2008**, *47*, 7396–7421; *Angew. Chem.* **2008**, *120*, 7506–7532; b) M. O. Senge, *Chem. Commun.* **2011**, *47*, 1943–1960; c) H. Yorimitsu, A. Osuka, *Asian J. Org. Chem.* **2013**, *2*, 356–373.
- [3] a) P. J. Chmielewski, L. Latos-Grażyński, *Coord. Chem. Rev.* **2005**, *249*, 2510–2533; b) I. Gupta, M. Ravikanth, *Coord. Chem. Rev.* **2006**, *250*, 468–518.
- [4] a) H. Segawa, K. Kunitomo, K. Susumu, M. Taniguchi, T. Shimidzu, *J. Am. Chem. Soc.* **1994**, *116*, 11193–11194; b) K. Susumu, K. Kunitomo, H. Segawa, T. Shimidzu, *J. Phys. Chem.* **1995**, *99*, 29–34.
- [5] a) A. Młodzianowska, L. Latos-Grażyński, L. Szterenber, *Inorg. Chem.* **2008**, *47*, 6364–6374; b) E. Pacholska-Dudziak, F. Ulatowski, Z. Ciunik, L. Latos-Grażyński, *Chem. Eur. J.* **2009**, *15*, 10924–10929.
- [6] a) Y. Matano, K. Matsumoto, Y. Nakao, H. Uno, S. Sakaki, H. Imahori, *J. Am. Chem. Soc.* **2008**, *130*, 4588–4589; b) Y. Matano, K. Matsumoto, H. Hayashi, Y. Nakao, T. Kumpulainen, V. Chukharev, N. V. Tkachenko, H. Lemmetyinen, S. Shimizu, N. Kobayashi, D. Sakamaki, A. Ito, K. Tanaka, H. Imahori, *J. Am. Chem. Soc.* **2012**, *134*, 1825–1839; c) K. Fujimoto, T. Yoneda, H. Yorimitsu, A. Osuka, *Angew. Chem. Int. Ed.* **2014**, *53*, 1127–1130; *Angew. Chem.* **2014**, *126*, 1145–1148.
- [7] a) Y. Matano, H. Imahori, *Acc. Chem. Res.* **2009**, *42*, 1193–1204; b) Y. Matano, T. Nakabuchi, T. Miyajima, H. Imahori, H. Nakano, *Org. Lett.* **2006**, *8*, 5713–5716; c) Y. Matano, T. Nakabuchi, S. Fujishige, H. Nakano, H. Imahori, *J. Am. Chem. Soc.* **2008**, *130*, 16446–16447; d) Y. Matano, M. Nakashima, T. Nakabuchi, H. Imahori, S. Fujishige, H. Nakano, *Org. Lett.* **2008**, *10*, 553–556; e) T. Nakabuchi, Y. Matano, H. Imahori, *Org. Lett.* **2010**, *12*, 1112–1115; f) Y. Matano, T. Nakabuchi, H. Imahori, *Pure Appl. Chem.* **2010**, *82*, 583–593; g) T. Nakabuchi, M. Nakashima, S. Fujishige, H. Nakano, Y. Matano, H. Imahori, *J. Org. Chem.* **2010**, *75*, 375–389.
- [8] a) A. Fukazawa, S. Yamaguchi, *Chem. Asian J.* **2009**, *4*, 1386–1400; b) Y. Matano, H. Imahori, *Org. Biomol. Chem.* **2009**, *7*, 1258–1271; c) Y. Ren, T. Baumgartner, *Dalton Trans.* **2012**, *41*, 7792–7800; d) T. Baumgartner, *Acc. Chem. Res.* **2014**, *47*, 1613–1622; e) M. Stolar, T. Baumgartner, *Chem. Asian J.* **2014**, *9*, 1212–1225.
- [9] T. Higashino, H. Imahori, *Chem. Eur. J.* **2015**, *21*, 13375–13381.
- [10] Crystallographic data for **12**: $\text{C}_{74}\text{H}_{53}\text{N}_8\text{PS}\cdot\text{C}_3\text{H}_8\text{O}\cdot 0.5(\text{C}_2\text{H}_4\text{Cl}_2)$, $M_r = 1226.84$, monoclinic, $C2/c$ (No.15), $a = 23.139(10)$, $b = 18.670(8)$, $c = 30.139(12)$ Å, $\beta = 90.068(11)^\circ$, $V = 13020(9)$ Å³, $\rho_{\text{calcd}} = 1.252 \text{ g cm}^{-3}$, $Z = 8$, $RI = 0.0836$ [$I > 2\sigma(I)$], $wR2 = 0.3069$ (all data), $\text{GOF} = 1.067$. CCDC 1495318 contains the supplementary crystallographic data for this paper. These data can be obtained free of charge from The Cambridge Crystallographic Data Centre.
- [11] a) A. Wakamiya, H. Nishimura, T. Fukushima, F. Suzuki, A. Saeki, S. Seki, I. Osaka, T. Sasamori, M. Murata, Y. Murata, H. Kaji, *Angew. Chem. Int. Ed.* **2014**, *53*, 5800–5804; *Angew. Chem.* **2014**, *126*, 5910–5914; b) W. Nakanishi, N. Matsuyama, D. Hara, A. Saeki, S. Hitosugi, S. Seki, H. Isobe, *Chem. Asian J.* **2014**, *9*, 1782–1785.

- [12] C. Ryppa, M. O. Senge, S. S. Hatscher, E. Kleinpeter, P. Wacker, U. Schilde, A. Wiehe, *Chem. Eur. J.* **2005**, *11*, 3427–3442.
- [13] a) 5,10,15,20-Tetra(4-tolyl)porphyrin ($\lambda_{\text{O}} = 647 \text{ nm}$ in CH_2Cl_2): S. Zakavi, S. Hoseini, *RSC Adv.* **2015**, *5*, 106774–106786; b) β - β' -bis[5,10,15,20-tetra(4-tolyl)porphyrin] ($\lambda_{\text{O}} = 655 \text{ nm}$ in CH_2Cl_2): G. Bringmann, D. C. G. Götz, T. A. M. Gulder, T. H. Gehrke, T. Bruhn, T. Kupfer, K. Radacki, H. Braunschweig, A. Heckmann, C. Lambert, *J. Am. Chem. Soc.* **2008**, *130*, 17812–17825.
- [14] a) Y. Matano, T. Miyajima, T. Fukushima, H. Kaji, Y. Kimura, H. Imahori, *Chem. Eur. J.* **2008**, *14*, 8102–8115; b) A. Saito, T. Miyajima, M. Nakashima, T. Fukushima, H. Kaji, Y. Matano, H. Imahori, *Chem. Eur. J.* **2009**, *15*, 10000–10004; c) Y. Matano, A. Saito, T. Fukushima, Y. Tokudome, F. Suzuki, D. Sakamaki, H. Kaji, A. Ito, K. Tanaka, H. Imahori, *Angew. Chem. Int. Ed.* **2011**, *50*, 8016–8020; *Angew. Chem.* **2011**, *123*, 8166–8170; d) Y. Dienes, M. Eggenstein, T. Kárpáti, T. C. Sutherland, L. Nyulászi, T. Baumgartner, *Chem. Eur. J.* **2008**, *14*, 9878–9889; e) Y. Ren, Y. Dienes, S. Hettel, M. Parvez, B. Hoge, T. Baumgartner, *Organometallics* **2009**, *28*, 734–740; f) H. Tsuji, K. Sato, Y. Sato, E. Nakamura, *J. Mater. Chem.* **2009**, *19*, 3364–3366; g) H. Tsuji, K. Sato, Y. Sato, E. Nakamura, *Chem. Asian J.* **2010**, *5*, 1294–1297; h) P.-A. Bouit, A. Escande, R. Szűcs, D. Szieberth, C. Lescop, L. Nyulászi, M. Hissler, R. Réau, *J. Am. Chem. Soc.* **2012**, *134*, 6524–6527; i) F. Riobé, R. Szűcs, P.-A. Bouit, D. Tondelier, B. Geffroy, F. Aparicio, J. Buendía, L. Sánchez, R. Réau, L. Nyulászi, M. Hissler, *Chem. Eur. J.* **2015**, *21*, 6547–6556.
- [15] J. Pommerehne, H. Vestweber, W. Guss, R. F. Mahrt, H. Bässler, M. Porsch, J. Daub, *Adv. Mater.* **1995**, *7*, 551–554.
- [16] a) J. C. Hummelen, B. W. Knight, F. LePeq, F. Wudl, J. Yao, C. L. Wilkins, *J. Org. Chem.* **1995**, *60*, 532–538; b) R. Tao, T. Umeyama, T. Higashino, T. Koganezawa, H. Imahori, *Chem. Commun.* **2015**, *51*, 8233–8236.
- [17] a) Y. Liu, J. Zhao, Z. Li, C. Mu, W. Ma, H. Hu, K. Jiang, H. Lin, H. Ade, H. Yan, *Nat. Commun.* **2014**, *5*, 5293; b) J. E. Anthony, A. Facchetti, M. Heeney, S. R. Marder, X. Zhan, *Adv. Mater.* **2010**, *22*, 3876–3892; c) J. L. Delgado, P.-A. Bouit, S. Filippone, M. Herranz, N. Martín, *Chem. Commun.* **2010**, *46*, 4853–4865; d) G. Li, R. Zhu, Y. Yang, *Nat. Photonics* **2012**, *6*, 153–161.
- [18] a) A. Saeki, Y. Koizumi, T. Aida, S. Seki, *Acc. Chem. Res.* **2012**, *45*, 1193–1202; b) A. Saeki, S. Seki, T. Takenobu, Y. Iwasa, S. Tagawa, *Adv. Mater.* **2008**, *20*, 920–923; c) H. Hayashi, W. Nishishi, T. Umeyama, Y. Matano, S. Seki, Y. Shimizu, H. Imahori, *J. Am. Chem. Soc.* **2011**, *133*, 10736–10739; d) Y. Matano, H. Ohkubo, Y. Honsho, A. Saito, S. Seki, H. Imahori, *Org. Lett.* **2013**, *15*, 932–935.

Received: August 1, 2016

Revised: August 20, 2016

Published online: September 9, 2016